Poster presented at the
Workshop on Stellar Structure:
Theory and Tests of Convective Energy Transport
Granada, Spain, September 30 - October 2, 1998

Treatment of the Superadiabatic Convection in Low-Mass Metal-Poor Stars from Realistic Hydrodynamics Simulations: Application to Globular Cluster Isochrones

Bernd Freytag[1,2], Maurizio Salaris[3], Hans-Günter Ludwig[1]

[1]Astronomical Observatory, NBIfAFG, Juliane Maries Vej 30, DK-2100 Copenhagen Ø, Denmark [bf@astro.ku.dk, hgl@astro.ku.dk]

[2]Institut für Theoretische Physik und Astrophysik der Universität Kiel, D-24098 Kiel, Germany

[3]Astrophysics Research Institute, Liverpool John Moores University, Liverpool L3 3AF, UK [ms@astro.livjm.ac.uk]

Abstract

For a grid of numerical 2D radiation hydrodynamics models of solar-like surface convection zones of metal-poor stars we calibrate the free parameter α of the mixing-length theory to give the same convective efficiency as the hydrodynamics models.

The calibrated α depends in a non-trivial way on the effective temperature, the gravity, and the metallicity. Nevertheless, isochrones of globular clusters resulting from evolutionary calculations based on the calibrated α have only an insignificant deviation (corresponding to an age-shift of some 0.1 Gyr) in the position of the turn-off compared to the standard case. A larger effect exists a the base of the red giant branch where the agreement between the locations of the theoretical and the observed isochrones is improved.

1 Numerical simulations

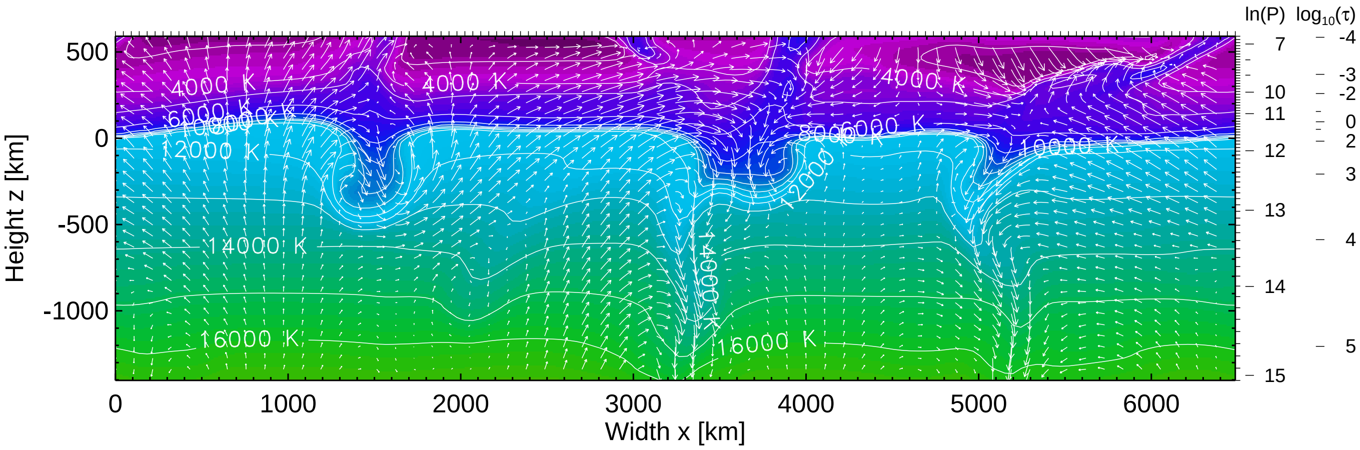

Figure 1: Snapshot of a main-sequence F star model (nt65g44n1) with $T_{\rm eff}$=6 500 K, log$g$=4.44, [M/H]=-1.0, 142×71 grid points, $v_{\rm max}\sim9.4$ km/s. It lies near the turn-off (TO) of a typical globular cluster isochrone.

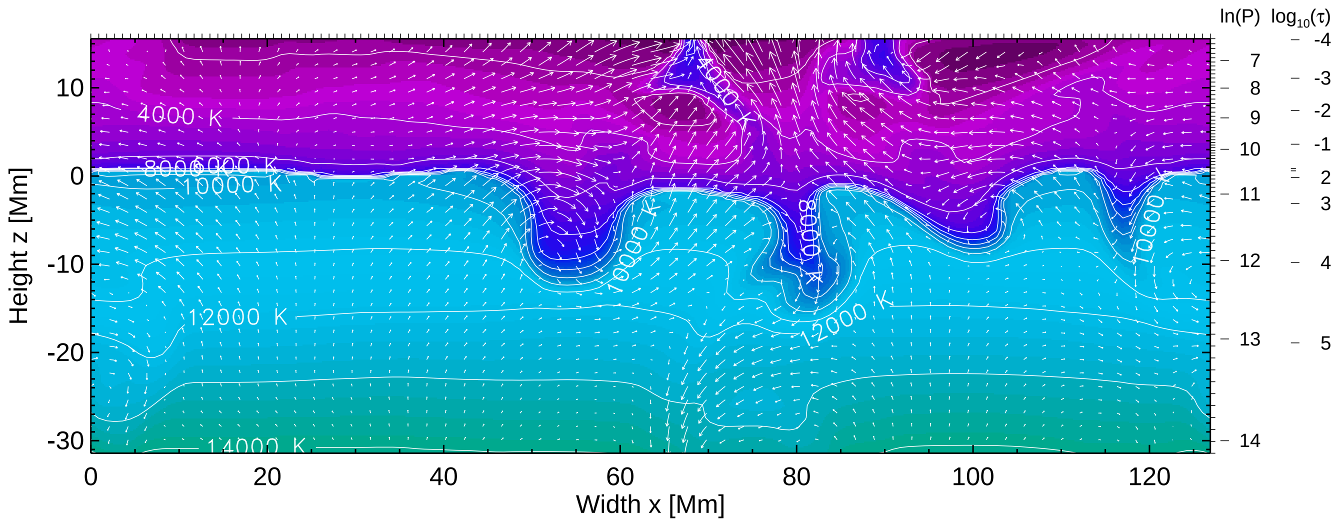

Figure 2: Snapshot of a model (nt50g29n1) with $T_{\rm eff}$=5 000 K, log$g$=2.94, [M/H]=-1.0, 142×71 grid points, $v_{\rm max}\sim14.6$ km/s. It lies near the base of the red giant branch (RGB) of a typical globular cluster isochrone.

With a 2D numerical radiation hydrodynamics (RHD) code (for details see Ludwig et al. 1994) a variety of models of stellar surface convection zones has been computed (see the poster of Ludwig, Freytag, Steffen). In the following, results for metal-poor stars with [M/H]=-1.0 and [M/H]=-2.0 are presented.

2 Flow fields

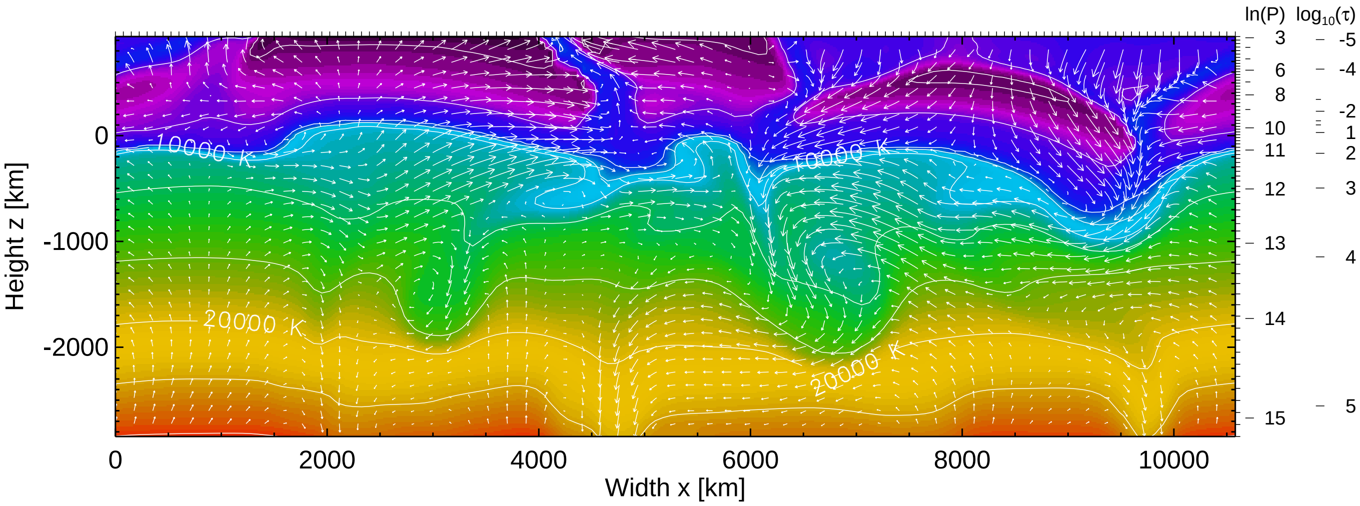

Figure 3: Snapshot of a main-sequence F star model (ot70g44n1) near the TO with T_{eff}=7 000 K, log$g$=4.44, [M/H]=-2.0, $142{\times}71$ grid points, $v_{\text{max}}{\sim}20$ km/s.

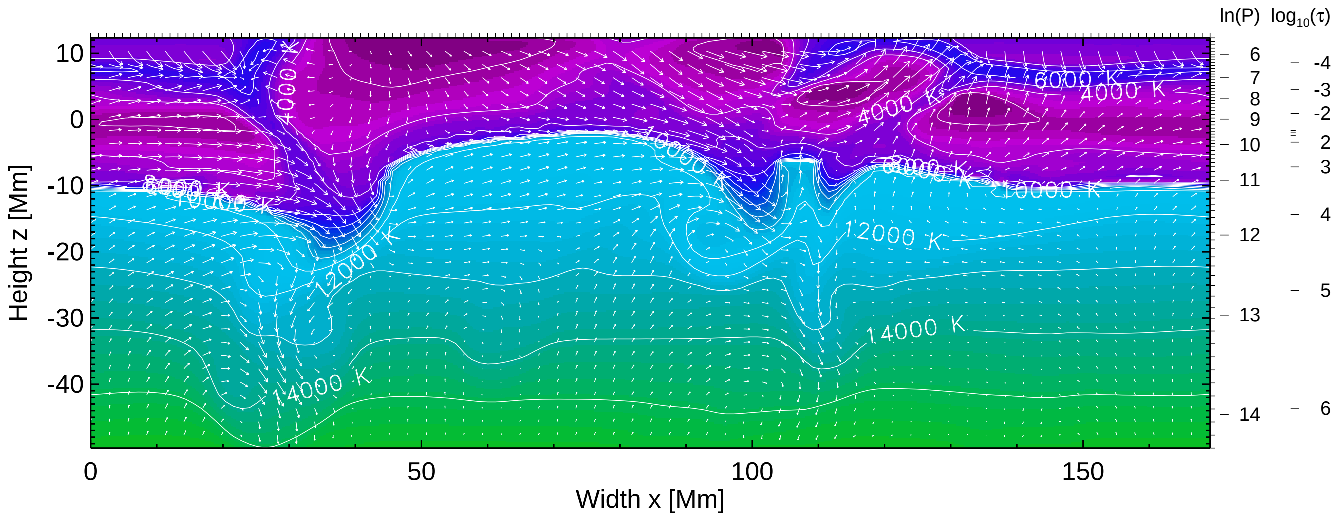

Figure 4: Snapshot of a model (ot55g29n1) near the base of the RGB with T_{eff}=5 500 K, log$g$=2.94, [M/H]=-2.0, $142{\times}71$ grid points, $v_{\text{max}}{\sim}16.6$ km/s.

Typical examples of convective flow patterns in stars near the turn-off (TO) and the base of the red giant branch (RGB) of globular cluster isochrones are presented in Figs. 1 to 4. The velocity field is indicated by short pseudo-streamlines. Contour lines and color show the temperature.

3 Calibration of the mixing-length parameter

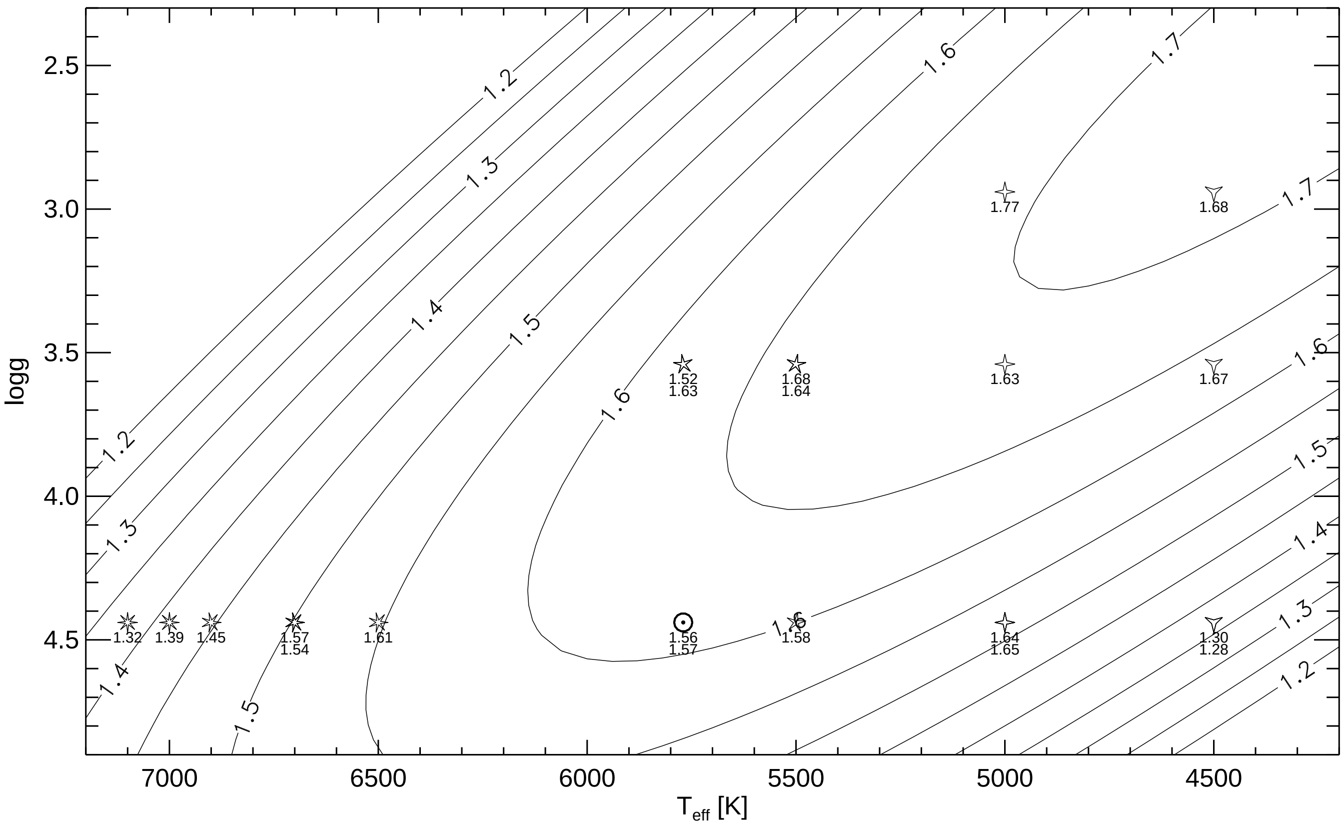

Figure 5: Calibrated mixing-length parameter α for [M/H]=-1.0 as function of effective temperature T_{eff} and gravity log$g$.

The free parameter α describing the mixing-length $\ell{=}\alpha H_p$ is adjusted to produce envelope models based on the mixing-length theory (MLT) with an entropy of the adiabatically stratified layers corresponding to the entropy of the material streaming into the RHD models from below. In this way an effective mixing-length parameter α is derived (see Steffen 1993 and Ludwig et al. 1998) for each T_{eff}/log$g$/[M/H] combination and plotted in Fig. 5 for [M/H]=-1.0 and Fig. 6 for [M/H]=-2.0 together with polynomial fits.

4 Variation of the mixing-length parameter

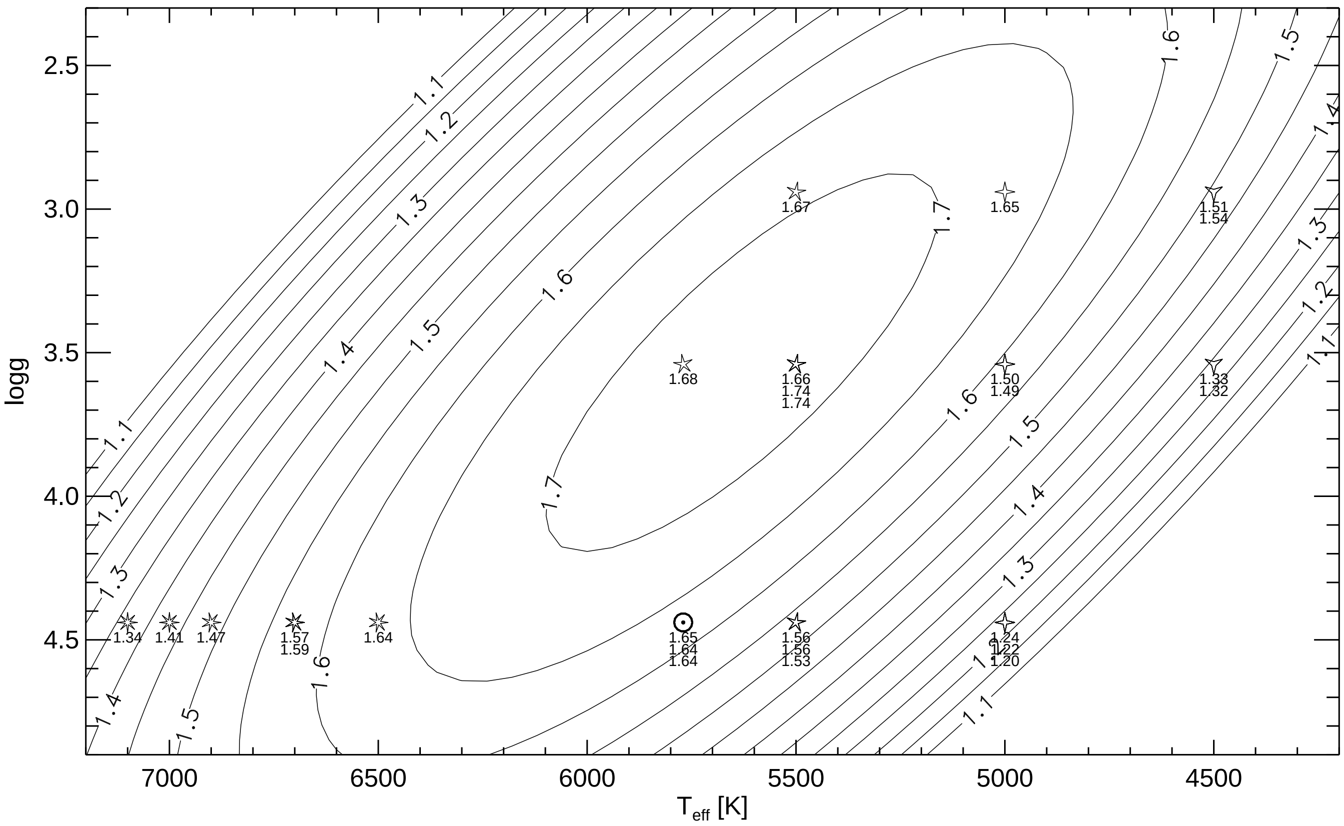

Figure 6: Calibrated mixing-length parameter α for [M/H]=-2.0 as function of effective temperature T_{eff} and gravity log$g$.

The behaviour of the calibrated mixing-length parameter α is similar for both metallicities: In a zone near the solar effective temperature and gravity α shows only a small variation. But there is a drop in α in the high-T_{eff}/low-log$g$ region and in the low-T_{eff}/high-log$g$ corner.

For solar metallicity the dependence of α is somewhat different (see the poster of Ludwig, Freytag, Steffen).

5 Computation of isochrones

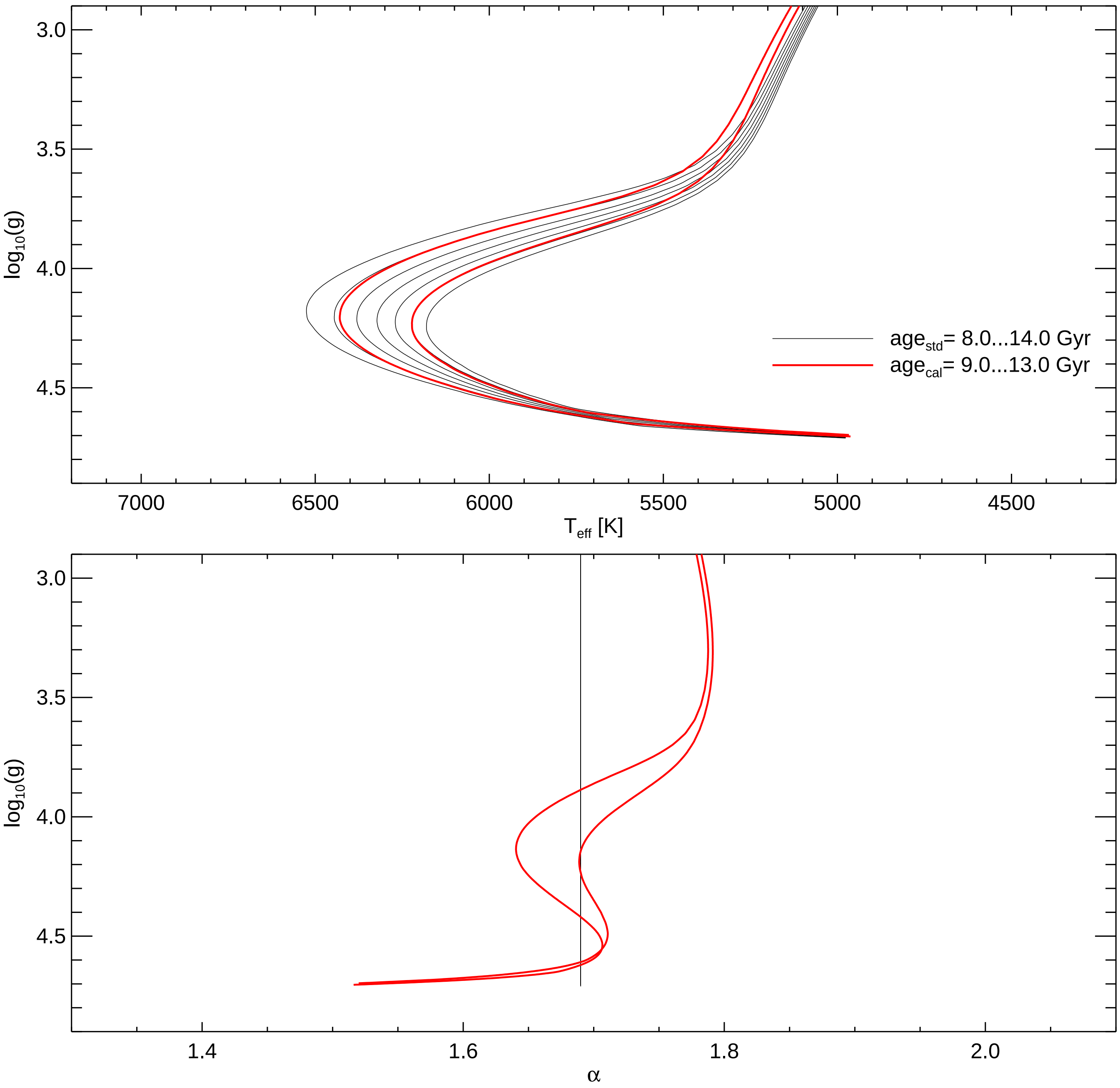

Figure 7: Top: isochrones in the $T_{\rm eff}/\log g$ diagram for [M/H]=-1.0. Two isochrones with calibrated α (age: 9, 13 Gyr) are compared to a sequence of standard isochrones with ages 8, 9, ... 14 Gyr. Bottom: mixing-length parameter α for the isochrones on top.

The evolutionary code used to compute the isochrones is described in Salaris et al. (1997). It employs a $T(\tau)$ relation closely resembling that of the RHD models. In the range of interest α has only an influence on the stellar radius (and thus the effective temperature and the surface gravity) for a fixed age, but not on the stellar luminosity. This allows an interpolation for a given α in a set of isochrones for a list of α-values. To improve the agreement with the Sun the calibrated α-values are scaled with a factor
$\alpha_\odot$(Fit to current Sun)/$\alpha_\odot$(RHD) $\sim$ 1.69/1.587 $\sim$ 1.065.

6 Isochrones with calibrated mixing-length parameter

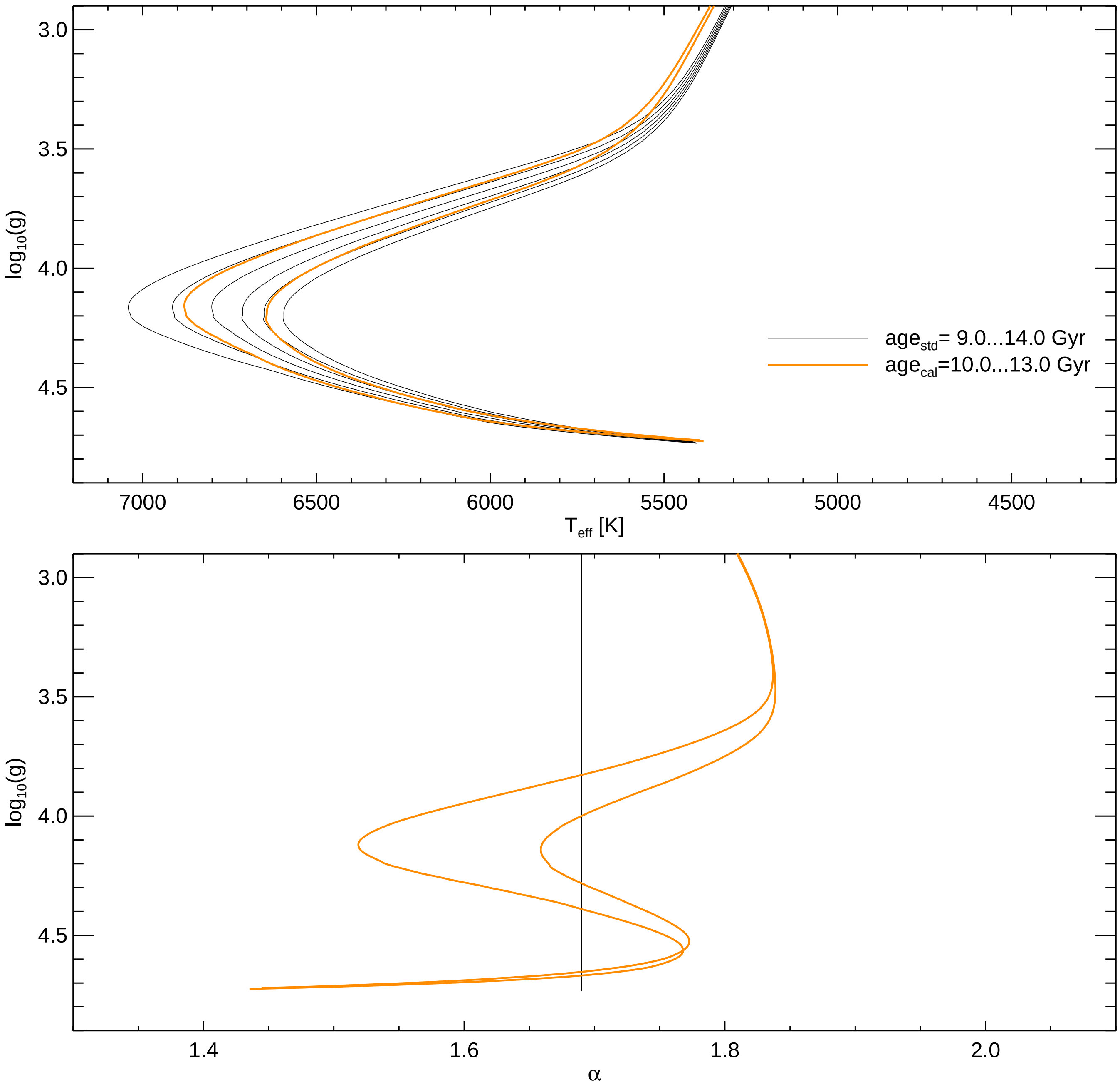

Figure 8: Top: isochrones in the $T_{\rm eff}$/log$g$ diagram for [M/H]=-2.0. Two isochrones with calibrated α (age: 10, 13 Gyr) are compared to standard isochrones with ages 9, 10, ... 14 Gyr. Bottom: mixing-length parameter α for the isochrones in the top panel.

In Fig. 7 and 8 a set of isochrones with constant α=1.69 is compared to a pair of isochrones with calibrated α. The run of the calibrated α along an isochrone is complex but the variation is moderate. On the main-sequence convection is very efficient – mostly independent of the exact value of α. Near the TO the isochrones do not reach the region in the $T_{\rm eff}$/log$g$-plane with the marked drop in α. At the base of the RGB the influence of the calibration is strongest. But even here it amounts only in an increase of the effective temperature of about 50 K.

7 Age-shift derived from the turn-off position for [M/H]=-1.0

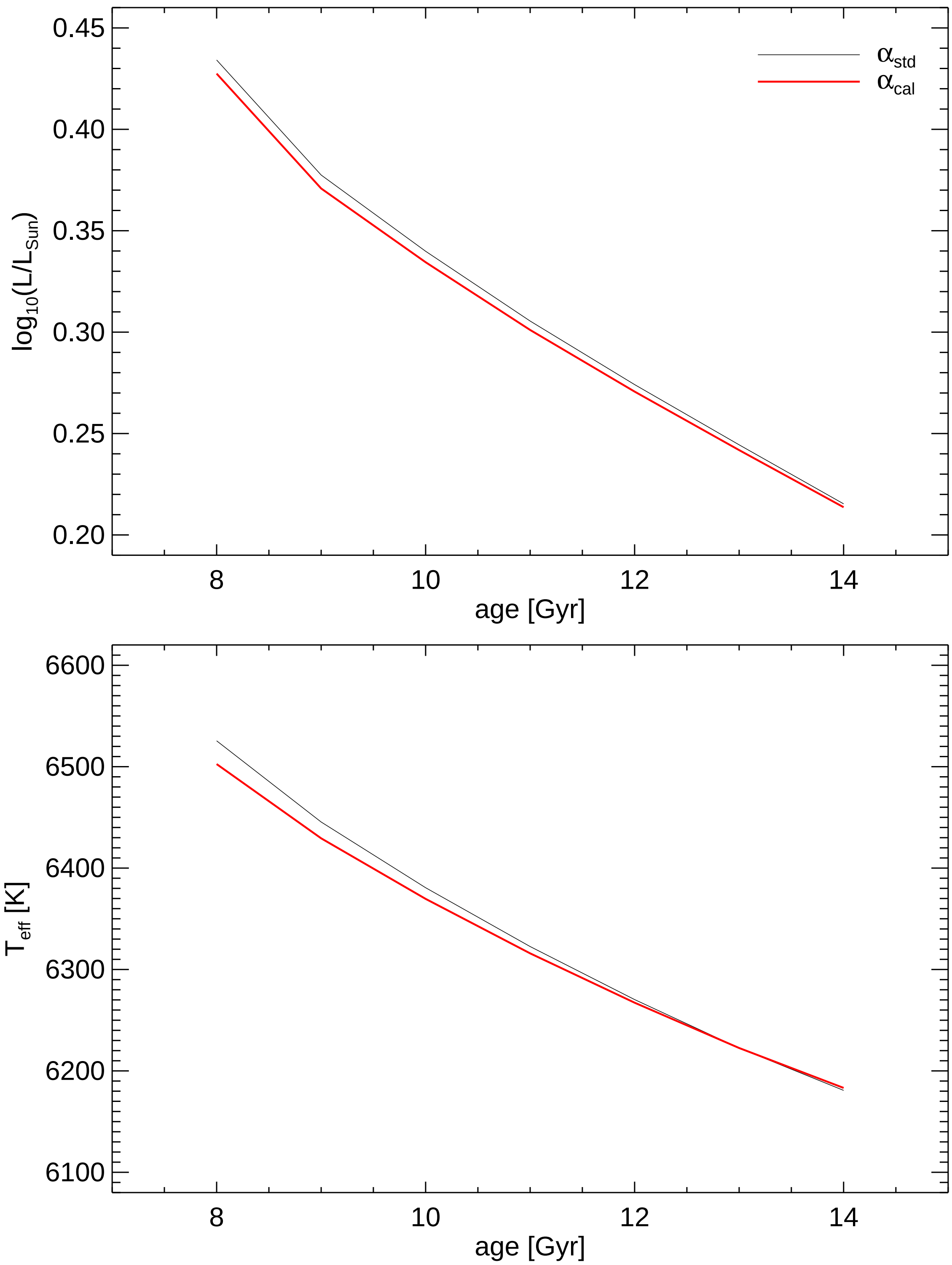

Figure 9: Top: luminosity of the TO versus age for isochrones with calibrated and constant α versus age for [M/H]=-1.0. Bottom: effective temperature of the TO versus age.

The horizontal difference between the curves in Figs. 9 and 10 gives the apparent age-shift of globular clusters if one uses theoretical isochrones with calibrated α instead of the standard ones to compare with the observed data.

For [M/H]=-1.0 the difference is non-zero only for very young clusters and even in this case the age of the clusters is reduced by just about 0.1 Gyr.

8 Age-shift derived from the turn-off position for [M/H]=-2.0

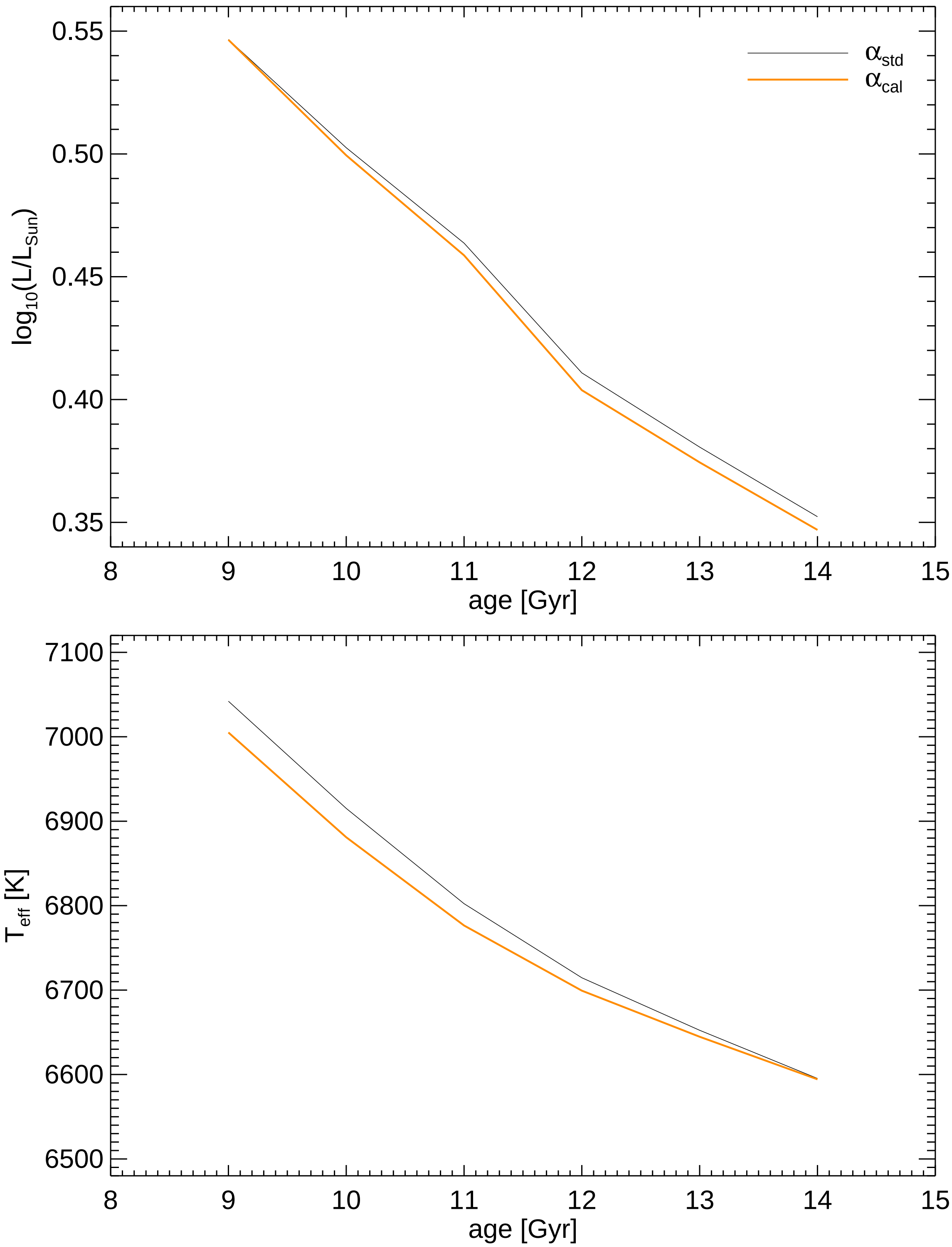

Figure 10: Top: luminosity of the TO versus age for isochrones with calibrated and constant α versus age for [M/H]=-2.0. Bottom: effective temperature of the TO versus age.

The apparent change of the age for [M/H]=-2.0 is with about 0.25 Gyr only slightly larger than for [M/H]=-1.0. It is still too small to cause a significant reduction of globular clusters ages.

9 Color-magnitude diagram of observed isochrones

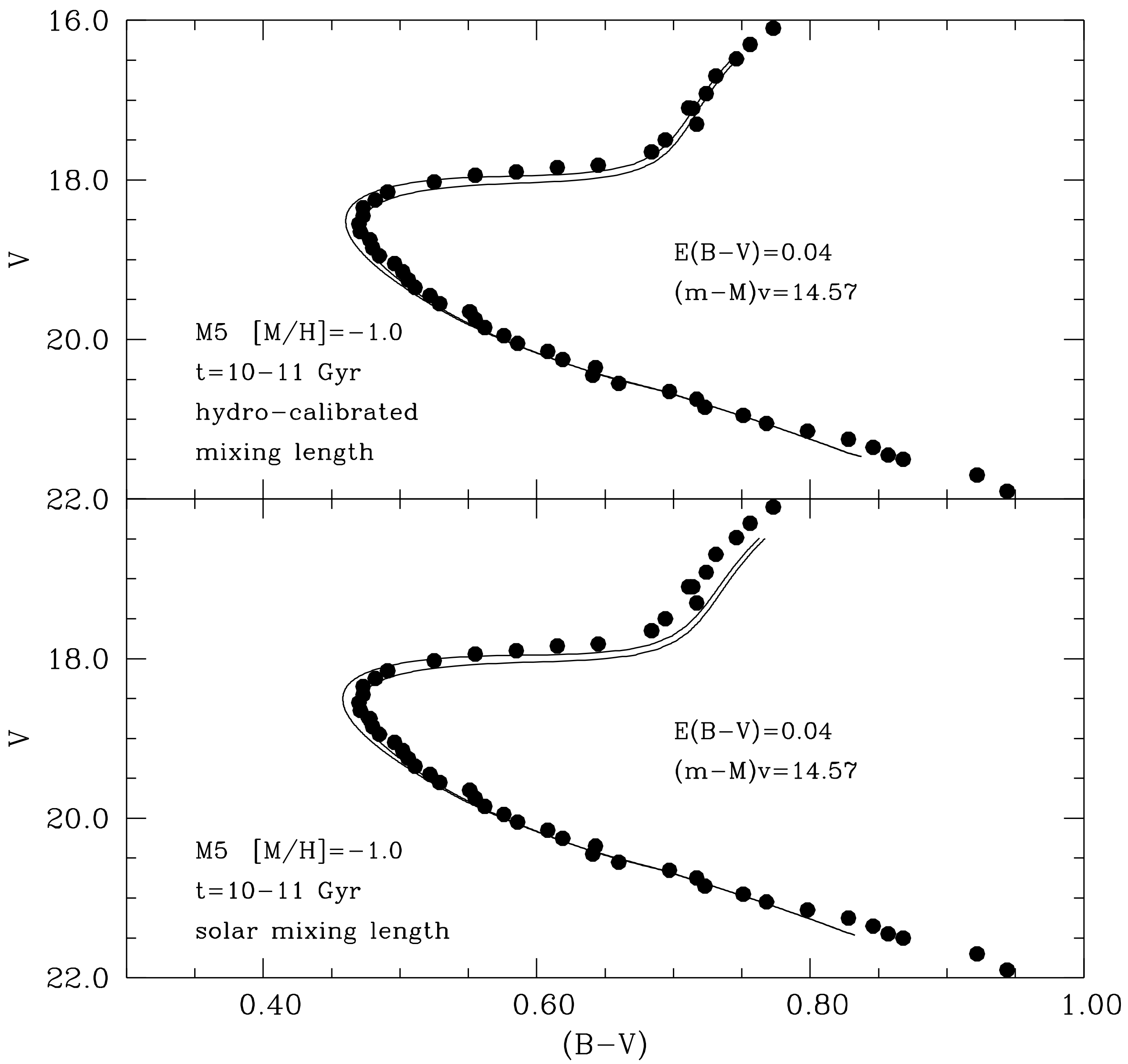

Figure 11: Theoretical and observed isochrones in color-magnitude diagrams for M5 ([M/H]=-1.0) with calibrated (top) and constant (bottom) α.

The theoretical isochrones are compared with observational data for M5 from Sandquist et al. (1996) in Fig. 11 and for M15 from Durrell & Harris (1993) in Fig. 12.

The metallicities are [Fe/H]=-1.11 (M5) and [Fe/H]=-2.12 (M15) as determined from high resolution spectroscopy by Carretta & Gratton (1997). Assuming [alpha/Fe]=0.3, this implies [M/H]$\sim$-0.9 for M5 and [M/H]$\sim$-1.91 for M15. The adopted distance scale comes from the results by Gratton et al. (1998). The color transformation is from Buser & Kurucz (1992).

10 Comparison of theoretical and observed isochrones

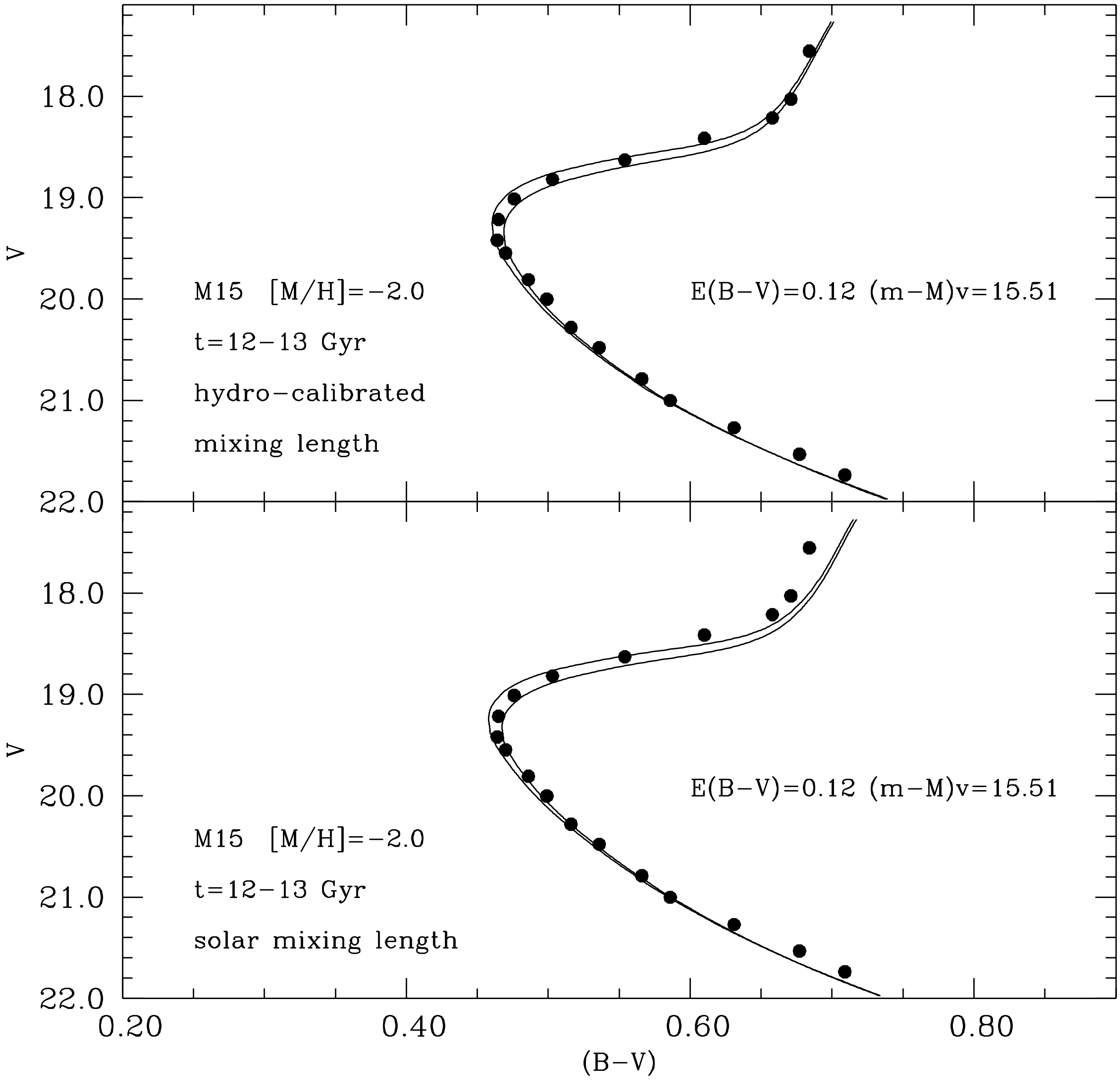

Figure 12: Theoretical and observed isochrones in color-magnitude diagrams for M15 ([M/H]=-2.0) with calibrated (top) and constant (bottom) α.

As it is clear from the preceeding analysis, the effects of the α calibration on the isochrones are rather subtle.

The most prominent effect is the improved agreement in the positions of the base of the RGB for the chosen color-transformation.

11 Conclusions

The calibrated mixing-length parameter α depends in a non-trivial way on effective temperature, gravity, and metallicity. Correspondingly, it exhibits complex variations along theoretical globular cluster isochrones.

But, observed globular cluster isochrones lie in ranges of the effective temperature and gravity where the calibrated mixing-length parameter α does not deviate significantly from its solar value.

For low metallicity ([M/H]=-2.0) the reduction of the apparent age derived from the effective temperature of the turn-off is only about 0.25 Gyr and even smaller for all other cases.

The position of the base of the red giant branch is shifted slightly towards higher effective temperatures by about 50 K which improves the agreement with the observed position in the color-magnitude diagram.

Deviations from the predictions of the mixing-length theory in the context of stellar evolution seem to be negligible for the age determination of globular clusters.

Acknowledgements

We would like to express our gratitude to Hartmut Holweger and Matthias Steffen for continuous support and helpful discussions. B.F. was supported by the *Deutsche Forschungsgemeinschaft, DFG* project Ho 596/36-1 and by the European *Training and Mobility of Researchers* Programme.

References

Buser R., Kurucz R., 1992, A&A 264, 557

Carretta E., Gratton R.G., 1997, A&AS 121, 95

Durrel P.R., Harris W.E., 1993, AJ 105, 1420

Gratton R.G., Carretta E., Clementini G., 1998, astro/ph 9808116.... (in press)

Ludwig H.-G., Freytag B., Steffen M., 1998, A&A (submitted): "A calibration of the mixing-length for solar-type stars based on hydrodynamical simulations"

Ludwig H.-G., Jordan S., Steffen M., 1994, A&A 284, 105

Salaris M., Degl'Innocenti S., Weiss A., 1997, ApJ 479, 665

Sandquist E., Bolte M., Stetson P.B., Hesser J.E., 1996, ApJ 470, 910

Steffen M., 1993, in "Inside the stars", IAU Coll. 137, eds. Weiss & Baglin, ASPCS 40, 300